Petroleum Science and Technology
Publication details, including instructions for authors and subscription information:
http://www.tandfonline.com/loi/lpet20

Synthesis and Characterization of Microporous Aluminophosphates of AFI Topology

R. W. Dorner [a] , N. J. Begue [a] , D. Y. Petrovykh [a] , D. R. Hardy [a] , F. W. Williams [a] , G. W. Mushrush [a b] & H. D. Willauer [a]

[a] Naval Research Laboratory , Washington , DC , USA

[b] George Mason University , Chemistry Department , Fairfax , Virginia , USA

Published online: 01 Apr 2014.

To cite this article: R. W. Dorner , N. J. Begue , D. Y. Petrovykh , D. R. Hardy , F. W. Williams , G. W. Mushrush & H. D. Willauer (2014) Synthesis and Characterization of Microporous Aluminophosphates of AFI Topology, Petroleum Science and Technology, 32:11, 1375-1382, DOI: 10.1080/10916466.2011.641652

To link to this article: http://dx.doi.org/10.1080/10916466.2011.641652

Petroleum Science and Technology, 32:1375–1382, 2014
ISSN: 1091-6466 print / 1532-2459 online
DOI: 10.1080/10916466.2011.641652

Synthesis and Characterization of Microporous Aluminophosphates of AFI Topology

R. W. Dorner,[1] N. J. Begue,[1] D. Y. Petrovykh,[1] D. R. Hardy,[1] F. W. Williams,[1] G. W. Mushrush,[1,2] and H. D. Willauer[1]

[1]*Naval Research Laboratory, Washington, DC, USA*
[2]*George Mason University, Chemistry Department, Fairfax, Virginia, USA*

Aluminophosphates of the AFI (aluminophosphate-5) topology were synthesized and characterized in order to study the influence of acid strength and distribution for the possibility of both conversion and selectivity for oligomerization reactions. It is well known that weaker acid sites lead to a product shift to hydrocarbons of lower carbon chain length and a lower conversion, and a reduction in acid site concentration has a similar effect. However, when a silylating agent modifies the surface acidity, the overall conversion drops, associated with a reduction in sticking probability of an olefin on the silicoaluminophosphate's (SAPO) crystal surface. This is associated with a reduced ability of the surface acid sites to crack the products upon exiting the internal pore system. This research reports on the synthesis and charactizeration of microporous aluminophates of AFI topology. *C*atalysts' properties were characterized by a series of spectroscopic and diffraction techniques, powder X-ray diffraction (XRD), X-ray photoelectron spectroscopy (XPS) and scanning electron microscopy (SEM). All catalysts were characterized in calcined form.

Keywords: AFI topology, aluminophosphate, jet fuel, oligomerization

1. INTRODUCTION

Microporous solid acid catalysts, namely, zeolites and aluminophosphates, are well known for their shape selectivity in catalysis reactions to produce higher hydrocarbons (Csicsery, 1984; Jones et al., 1998; Thomas et al., 2001; Dorner et al., 2008, 2009; Roldan et al., 2007; Laugier and Bochu, 2003; Toby, 2001; Chao et al., 1992; Hartmann and Kevan, 1999; Hedge et al., 1988; Dumitriu et al., 2002). The U.S. Navy's interest in this process arises from its high consumption of jet fuel, 2.2 million gallons/day; it is therefore of interest to produce long-chain hydrocarbons in the jet fuel range, C_9–C_{16}, (Dorner et al., 2009). Zeotype material properties such as pore size, channel structure, as well as the strength and number of Brønsted acid sites can be tailored to match the desired properties for the specific reaction (Dorner et al., 2008). AFI (aluminophosphate-5) topology was chosen for this study to examine the impact of the addition of heteroatoms such as silicon or cobalt on the synthesis gel, which changes the material's Brønsted acidity. Furthermore, when substituting Si into the parent AFI framework, adjustments made to the pH of the synthesis gel leads to a modification

Address correspondence to Heather D. Willauer, Naval Research Laboratory, Code 6183, 4555 Overlook Avenue, SW, Washington, DC 20375. E-mail: heather.willauer@nrl.navy.mil

Color versions of one or more of the figures in the article can be found online at www.tandfonline.com/lpet.

TABLE 1
XPS Electron Atomic Composition (obs. at%) Results of the Calcined SAPO-5 (pH 8.5) and the Silylated SAPO-5 (pH 8.5) Samples Compared to the As-Expected Bulk Composition ($Si_{0.1}Al_1P_{0.9}O_4$)

Peak Assignment	*Area*	*obs. At%*	*bulk at%*
SAPO-5(pH 8.5)			
Si 2p	14.5	2.2	1.6
Al 2p	110.6	16.4	16.7
O 1s	447.2	66.4	66.7
P 2p	101.4	15.1	15.0
Sum	673.7	100.0	100.0
SAPO-5(pH 8.5) sylilated			
Si 2p	63.2	8.2	1.6
Al 2p	110.2	14.3	16.7
O 1s	489.6	63.7	66.7
P 2p	105.1	13.7	15.0
Sum	768.1	100.0	100.0

in the number of acid sites, with a high pH leading to the suppression of silicon island formation (Roldan et al., 2007). Based on the product distribution, the AFI system can yield great insights into the importance of the number of acid sites as well as the acid strength on the oligomerization reaction of alkenes to longer chain hydrocarbons. However, the objective of this study is not to develop a suitable catalyst for the conversion of alklenes to hydrocarbons in the jet fuel range. Instead, we are trying to understand and optimize the underlying characteristics needed for an effective catalyst in this reaction, using the AFI framework as a model system.

1.1. Experimental Conditions and Methods

All chemicals, unless otherwise noted, were purchased from Sigma-Aldrich Chemical Company (Milwaukee, WI).

1.2. Catalyst Preparation

All of the microporous materials of AFI topology were synthesized using conventional hydrothermal methods, using *N*-methyl-dicyclohexylamine as a structure-directing agent (SDA). The different AFI topologies were synthesized by adding cobalt acetate in the CoAPO-5 cases, or silicate (tetraethyl orthosilicate) for the SAPO-5 synthesis, to an aqueous solution of phosphoric acid, which was followed by the addition of aluminum hydroxide. After rigorous stirring for ca. 10 min, the gel attains homogeneity, and the organic template, *N*-methyldicyclohexylamine, was added to form the final gel. After the gel was stirred for ca. 1 hr, it was transferred to a Teflon-lined autoclave, which was heated in a preheated oven at 423 K for ca. 16 hr. The solids extracted by conventional filtering and drying procedures were checked for phase purity by X-ray diffraction (XRD). SAPO-5 was synthesized with the synthesis gel having a pH of 7 and 8.5, achieved through the addition of different concentrations of SDA (henceforth referred to as SAPO-5 [pH 7] and [pH 8.5], respectively). Synthesis conditions and gel composition are summarized in Table 1 for all AFI materials. Subsequent to collecting the material it was calcined in air at 808 K for 8 hr to remove the organic SDA.

In addition to being tested in its calcined form, SAPO-5 (pH 8.5) was tested after being silylated. The glassware was initially dried at 373 K for 1 hr, and the solvent (toluene) was dried over Drierite

(W.A. Hammond Drierite Co. Ltd.) to remove the water present. The glassware was subsequently exposed to a 0.1 vol% tributylchlorosilane dried toluene mixture for 12 hr to cap all silanol groups present on the glassware. Having treated the round-bottomed flask, 50 mL of dried toluene and 5 g of calcined SAPO-5 (pH 8.5) was placed in it. The solution was stirred and heated to 348 K for 30 min while being purged with ultra-high-purity He. Two milliliters of tributylchlorosilane were added to the mixture through a rubber septum and was left to stir for 2 hr. The silylated SAPO was collected through conventional filtering methods and washed three times with dried toluene and subsequently dried for 2 hr at 373 K.

1.3. Powder X-ray Diffraction

Powder XRD measurements were performed on all materials. The data were collected on a D8 Siemens Bruker diffractometer with a general area detector employing the Bragg-Brentano geometry and the CuK_α1 wavelength. The data were collected in the 5–50° 2θ range with a step increment of 0.01°; the time for each step was 2 s. The data were visualized using Celref3 software (Laugier and Bochu, 2003). LeBail fits were performed on the XRD data collected, employing GSAS EXPGUI software (Toby, 2001). The patterns were analyzed in space group *P6cc* and unit cell dimensions as reported by Chao et al. (1992).

1.4. X-ray Photoelectron Spectroscopy

X-ray photoelectron spectroscopy (XPS) was used to assess the surface species and quantities present on the powder particles. The XPS studies were carried out using a K-Alpha instrument (Thermo Scientific, UK) and Unifit software (Hedge et al., 1988) for data analysis, using the instrument-specific powder sample (Laugier and Bochu, 2003).

The system base pressure was less than 5×10^{-9} mbar; however, the pressure in the analysis chamber during data collection and analysis was 2×10^{-7} mbar due to the use of the low-energy dual-beam flood gun for charge neutralization. A monochromated Al K_α ($h\nu = 1{,}486.6$ eV $\pm$ 0.2) was used as the X-ray source. The instrument is regularly calibrated to the binding energies (BEs) of Au, Cu, and Ag peaks. The O 1s BE is used as internal standard.

1.5. Scanning Electron Microspcopy

Structural and chemical characterization was performed with a field emission scanning electron microscope (FESEM; model LEO DSM 982, LEO). The scanning electron microscope (SEM) was operated at an accelerating voltage of 5 kV and the working distance was varied from 3 to 8 mm. The powder was placed under the SEM detector as a loosely scattered powder stuck to conducting tape. All images are a good representation of the overall bulk material.

1.6. Brunauer-Emmett-Teller Surface Area Measurements

Brunauer-Emmett-Teller surface areas were measured using a Micromeritics ASAP2010 accelerated surface area and porosimetry system. An appropriate amount (~0.25 g) of catalyst sample was taken and slowly heated to 200°C for 10 hr under a vacuum (~50 mTorr). The sample was then

transferred to the adsorption unit, and the N_2 adsorption was measured at the boiling temperature of nitrogen.

2. RESULTS AND DISCUSSION

2.1. AFI Synthesis and Characterization

T-atoms (i.e., Al^{3+} and P^{5+}) within aluminophosphates can be replaced with different heteroatoms (Hartmann and Kevan, 1999). When one replaces a trivalent Al with a divalent Co or the P^{5+} with an Si^{4+}, charge compensation occurs via a Brønsted acid site (Hartmann and Kevan, 1999). The strength of the formed Brønsted acid site depends on the choice of heteroatom, with the strength of the acid site having been confirmed in several temperature-programmed desorption studies for the system investigated in this study (Hedge et al., 1988; Dumitriu et al., 2002; Dorner et al., 2008). Furthermore, when one replaces phosphorus in the AlPO structure with Si, changing the pH of the synthesis gel can lead to a difference in silicon distribution. The structure formed at lower pH displays a higher concentration of silicon islands throughout the material and subsequently a reduced number of acid sites (Roldan et al., 2007). We are thus able, through tailoring the synthesis conditions, to alter the acid strength (SAPO > CoAPO) as well as the number of acid sites (SAPO-5 [pH 8.5] > SAPO-5 [pH 7]) present in the solids.

All of the as-synthesized AFI structures were characterized for phase purity employing XRD and morphology were determined through SEM images. The XRD patterns of all three AFI phases investigated (CoAPO-5; SAPO-5, pH 7; and SAPO-5, pH 8.5) are identical and show no impurity peaks in the as-synthesized form. The histograms correlate well with the expected XRD pattern for the AFI topology. It displays a one-dimensional channel (i.e., channels running in one direction without intersecting each other) of 7.3 Å in diameter. After calcination, which removes the organic SDA from the framework, the AFI topologies do not show a loss of structural integrity, remaining intact with no changes in symmetry observed (Figure 1; space group: *P6cc*, $a = 13.74$; $c = 8.36$) and are in good agreement with results reported elsewhere (Chao et al., 1992). A successful LeBail fitting was performed on the XRD pattern of the calcined SAPO-5, pH 8.5 sample, yielding a satisfactory χ^2 value of 1.8 (Figure 1). SEM images taken of the materials display crystallites made up of staked hexagonally shaped platelets, giving rise to particles with a spherical appearance. All of the different AFI materials are composed of particles of identical morphology with particle sizes ranging between 5 and 10 μm in diameter. Brunauer-Emmett-Teller measurements yielded surface areas of $\sim$300 m^2/g and micropore volumes of $\sim$0.10 cc/g for all samples. As a comparison, micropore volume was observed for both the sylilated as well as the unsylilated sample, and we can conclude that the pore mouths were not blocked by the surface modification agent. Microporous materials have acid sites both in the channel system as well as on the material's surface. Acid sites on the surface, however, do not have the advantage of shape selectivity that the sites within the channels display. After the products exit the pore systems of the AlPOs, the acid sites on the crystallite surfaces can contribute to cracking of the formed long-chain HC[20]; consequently, the SAPO-5 (pH 8.5) was silylated with tributylchlorosilane to mitigate the effect that surface acid sites play on the overall reaction. Tributylchlorosilane was too large in diameter to fit into the AFI channel system and thus was chosen as the capping agent.

To establish whether the silylation process was successful, XRD, SEM, and XPS analytical techniques were employed. The XRD histogram of the silylated AFI topology displays an XRD pattern, which is identical to that of the calcined sample (Figure 2), indicating that the silylating agent does not form an amorphous silica phase during the treatment. One would expect to observe an amorphous contribution (i.e., increased background) in the XRD pattern if the silylating agent had agglomerated and formed an amorphous phase instead of capping the surface acid sites during the silylating

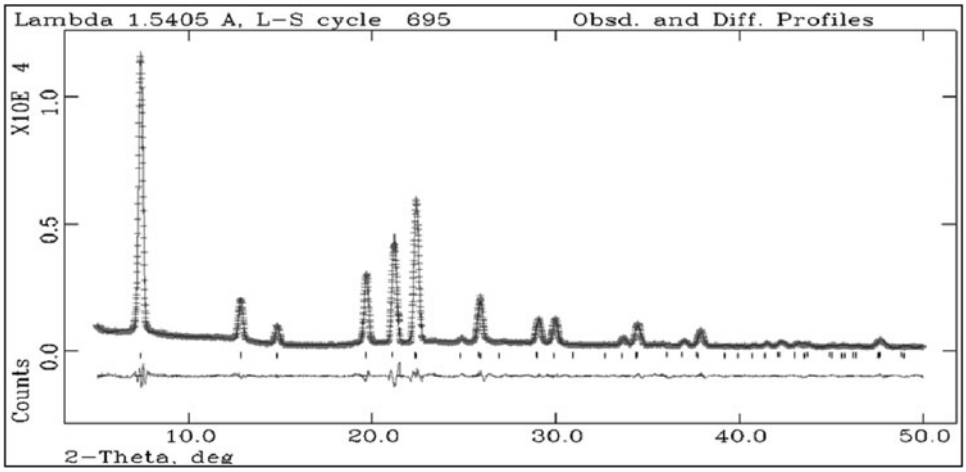

FIGURE 1 Experimental powder diffraction data (crosses) and simulated XRD pattern (solid line) obtained after performing the LeBail fitting to the XRD data and the difference profile (displayed below the previous mentioned plots) of the calcined SAPO-5 (pH 8.5). The diffraction pattern was fitted using the space group *P6cc* and yielded unit cell dimensions of $a = 13.74$, $c = 8.36$ with the fitting parameter $\chi^2 = 1.8$. No crystalline impurities of significant amounts (above detection limit) were present in the powder, and the framework showed complete integrity.

process. SEM images corroborate that the silylation process was successful because the silylated sample shows a visible modification of the crystallite's surface. One can detect small alterations on the surface that are not present in the untreated sample (Figures 3a and 3b, respectively), indicating that the treatment was successful in capping the crystallites' surface acid sites. Furthermore, the silylation process does not seem to have a detrimental effect on the overall integrity of the AlPO framework (as seen in the unaltered XRD and SEM images after treatment).

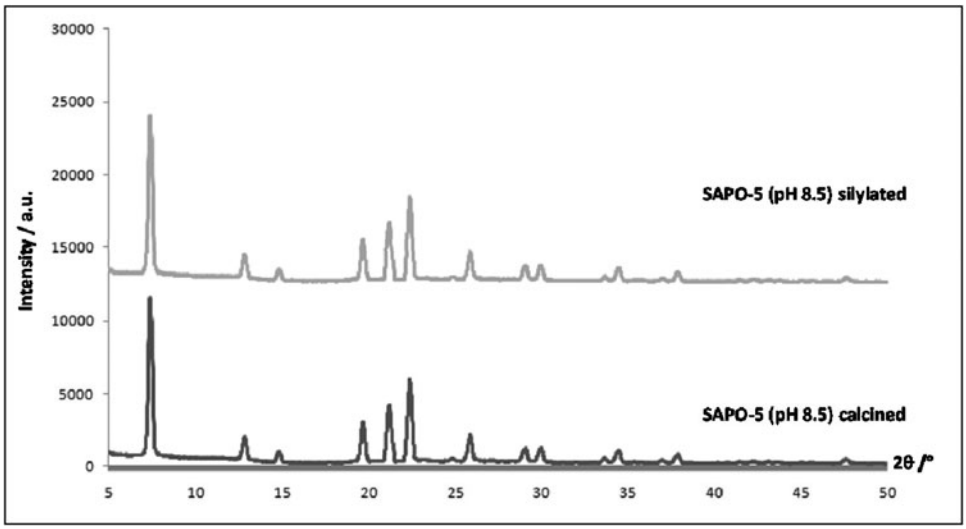

FIGURE 2 XRD of SAPO-5 (pH 8.5) both calcined and silylated. It can be seen that the silylation process did not lead to a disintegration or alteration of the AFI framework.

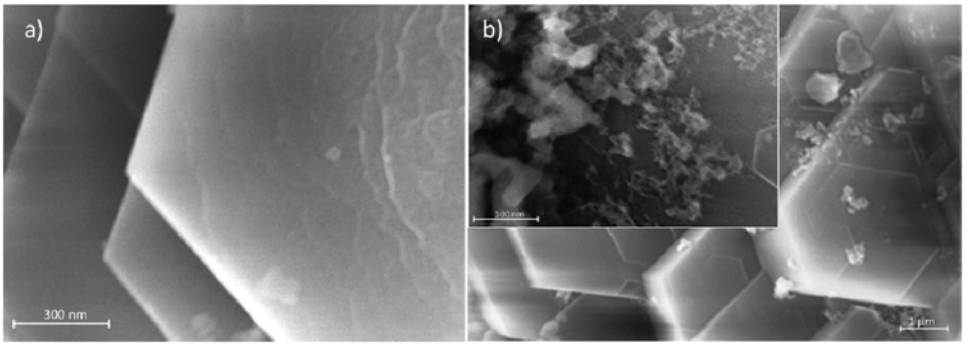

FIGURE 3 SEM images of (a) untreated and (b) silylated SAPO-5 (pH 8.5) crystal surfaces (magnifications are given on the image). At the higher magnification with the silylated sample one can distinguish a modification of the surface by the silylating agent, whereas the as-synthesized one displays clean and smooth surfaces.

XPS data were collected on the silylated and unsilylated samples to corroborate that the treatment was successful. The untreated SAPO displayed a surface composition that was very similar to the expected bulk chemical composition of the framework; that is, $AlSi_{0.1}P_{0.9}O_4$ (Table 1). The silylated sample, on the other hand, exhibited a significant increase in Si surface species, as one would expect, due to the presence of surface-grafted $Si(C_4H_9)_3$ groups, by a factor of 2.7, as shown in Table 1. As the XPS technique penetrates deeper than just the external surface of the aluminophosphates, it must be noted that the actual surface silicon concentration might be higher than that measured by XPS. The Si 2p peak of the silylated sample can be deconvoluted into two doublets, with the one at higher BE associated with the SiO_2 units present in the AFI framework and the one at the lower BE

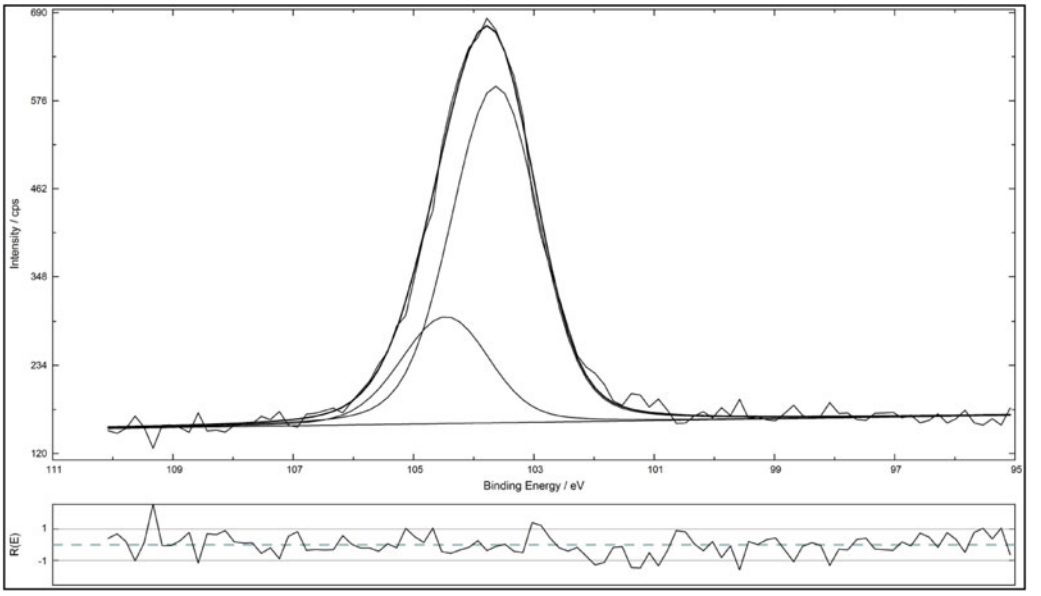

FIGURE 4 XPS Si 2p peak of the silylated SAPO-5 (pH 8.5). The Si 2p doublet can be deconvoluted into two peaks, with the one at lower BE associated with the surface silane and the one at higher BE arises due to the SiO_2 units within the AFI framework.

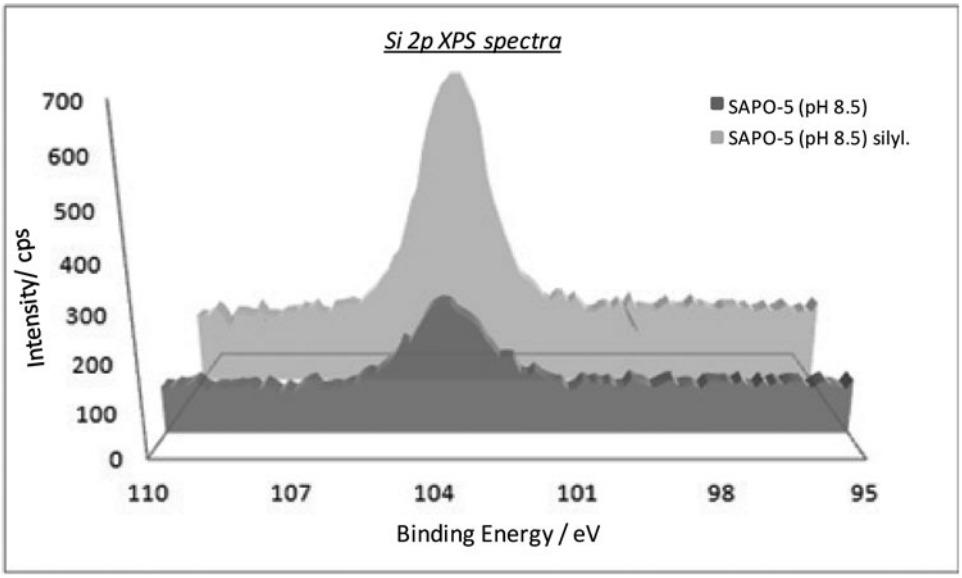

FIGURE 5 XPS peaks of the silylated and unsilylated SAPO-5 (pH 8.5), displaying a clear increase in Si-surface species after the silylation process.

associated with the surface silane groups resulting from their respective oxidation states, namely, SiO_2 and SiO (Figure 4). The ratio of the silane to the silica peak (3:1; Figure 5) relates well to the increase in the Si weight distribution (2.7:1) in the material after silylation (Table 1). Phase purity as well as morphology of all AFI materials was determined with XRD and SEM. Furthermore, surface modification by a silylating agent was established to have been successful via XRD, SEM, and XPS.

3. CONCLUSIONS

Based on this study, it is possible to synthesize an ideal solid acid catalyst for the study of oligomerization reactions, namely, a zeolite with strong acid sites and a low Si/Al ratio. Capping of the aluminophosphate's surface acid sites by a silylating agent may lead to a shift to longer chain hydrocarbons. This could be achieved by suppressing the cracking of the products. Future studies including ethylene feedstock and a mixture of olefins as well as investigating the influence of pore size will also be reported.

FUNDING

This work was supported by the Office of Naval Research both directly and through the Naval Research Laboratory.

REFERENCES

Chao, K. J., Sheu, S. P., and Sheu, H. S. (1992). Structure and chemistry of cobalt in CoAPO-5 molecular sieve. *Faraday Trans*. 88:2949–2954.

Csicsery, S. M. (1984). Shape-selective catalysis in zeolites. *Zeolites* 4:202–213.

Dorner, R. W., Deifallah, M., Catlow, C. R. A., Cora, F., Elangovan, S. P., Okubo, T., and Sankar, G. (2008). Heteroatom-substituted microporous AFI and ATS structured materials for hydrocarbon trap: An insight into the aluminophosphate framework–toluene interaction. *J. Phys. Chem. C* 112:4187–4194.

Dorner, R. W., Hardy, D. R., Williams, F. W., Davis, B. H., and Willauer, H. D. (2009). Influence of gas feed composition and pressure on the catalytic conversion of CO_2 to hydrocarbons using a traditional cobalt based Fischer-Tropsch catalyst. *Energ. Fuel.* 23:4190–4195.

Dumitriu, E., Guimon, C., Hulea, V., Lutic, D., and Fechete, I. (2002). Transalkylation of toluene with trimethylbenzenes catalyzed by various AFI catalysts. *Appl. Catal. Gen.* 237:211–221.

Hartmann, M., and Kevan, L. (1999). Transitional-metal ions in aluminophosphate and silicoaluminumphosphate molecular sieves: Location, interaction with adsorbate and catalytic properties. *Chem. Rev.* 99:635–663.

Hedge, S. G., Ratnasamy, P., Kustov, L. M., and Kazansky, V. B. (1988). Acidity and catalytic activity of SAPO-5 and AlPO-5 molecular sieves. *Zeolites* 8:137–141.

Jones, C. W., Tsuji, K., and Davis, M. E. (1998). Molecular sieve catalysts for the regioselective and shape-selective catalysts. *Nature* 393:52–60.

Laugier, J., and Bochu, B. C. (2003). Available at: http://www.ccp14.ac.uk/tutorial/lmgp/celref.htm

Roldan, R., Sanchez-Sanchez, M., Sankar, G., Romero-Salguero, F. J., and Jimenez-Sanchidrian, C. (2007). Influence of pH and Si content on Si incorporation in SAPO-5 and their catalytic activity for isomerization of n-heptane over Pt loaded catalysts. *Microporous and Mesoporous Materials* 99:288–298.

Thomas, J. M., Raja, R., Sankar, G., and Bell, R. G. (2001). Molecular sieve catalysts for the regioselective and shape-selective oxyfunctional of alkanes in air. *Accounts Chem. Res.* 34:191–200.

Toby, B. H. (2001). EXPGUI, a graphical user interface for GSAS. *J. Appl. Crystallogr.* 34:210–213.